

Predicted Energy Resolution of a Running-Sum Algorithm for Microcalorimeters

Bradley K. Alpert · W. Bertrand Doriese ·
Joseph W. Fowler · Joel N. Ullom

Received: 19 July 2011 / Accepted: 17 November 2011
© Springer Science+Business Media, LLC (outside the USA) 2011

Abstract The energy resolution of a high-pulse-rate filtering algorithm recently introduced by Hui Tan *et al.*, based on running sums of TES microcalorimeter output streams, is predicted from average pulse shape and noise autocovariance. We compare with empirical resolution, and with optimal filtering predicted and empirical resolution, for a ^{55}Fe source measured by multiplexed 2×4 , 2×8 , and 2×12 arrays of microcalorimeters.

Keywords Filter algorithms · High-rate processing · Microcalorimeter · Uncertainty

1 Introduction

One recent approach to cope with the data output of increasingly large arrays of microcalorimeters, proposed to reduce offline processing and storage requirements, to increase throughput by rejection of fewer piled-up pulses, and to simplify processing, is a set of algorithms due to Hui Tan *et al.* [1–3] that relies on running sums of the data streams. We predict the energy resolution of the most recently reported algorithm [3], based on analysis involving the average pulse and noise autocovariance, and compare to both the empirical resolution of the algorithm and the predicted and empirical resolution for optimal filtering of transition-edge-sensor (TES) microcalorimeter measurement of a ^{55}Fe source for the 5.9 keV MnK_α complex recorded in the spring of 2008 for Constellation-X/IXO technology demonstrations.

Contribution of U.S. government, not subject to copyright in the United States.

B.K. Alpert (✉) · W.B. Doriese · J.W. Fowler · J.N. Ullom
National Institute of Standards and Technology, 325 Broadway, Boulder, CO 80305, USA
e-mail: alpert@boulder.nist.gov

2 Processing Algorithm

The algorithm [3] subtracts the height of the baseline from the height of a pulse on top of the baseline. The pulse height is determined from a running sum of L_{RS} signal samples, recorded at the position where the sum reaches its maximum. The baseline is determined, asynchronously from the pulse height, as the average value of a running sum of L_B signal samples. Each of these running sums is obtained from samples taken at times free of other pulses, through latches timed from pulse triggers [3].

Reduction of pile-up losses is enabled by L_{RS} being quite short (here for samples spanning less than 1 ms), so that a second pulse does not spoil a pulse being recorded even if the second arrives rather shortly after the first. The second pulse would, however, be discarded. In addition, the much greater length of L_B (greater than 100 ms) is not especially restrictive, due to its collection being asynchronous from that of the pulses.

3 Analysis Method

3.1 Signal and Noise Model

3.1.1 Continuous Model

We assume a signal f consisting of a single pulse sitting on a baseline

$$f(t) = A \cdot S(t - t_0) + B,$$

where S is the pulse shape and A and B are the heights of the pulse and baseline. For notational convenience, the time t_0 of pulse arrival is henceforth zero. A noisy signal consists of signal plus noise $m(t) = f(t) + \eta(t)$, where the noise η is assumed to be a realization of a stationary stochastic process with zero mean and autocovariance

$$R_\eta(\tau) = \int_{-\infty}^{\infty} \eta(t)\eta(t + \tau)dt.$$

3.1.2 Discrete Model

The measurement apparatus obtains an approximation m_i of $m(i\Delta)$ for $i \in \mathbb{Z}$, where Δ is the time spacing between samples, as a convolution of m with a response function

$$m_i = \int_{-\infty}^{\infty} m(i\Delta - t)w(t)dt,$$

where we assume w is an approximate δ -function centered at the origin with unit integral. We define f_i , s_i , and η_i analogously for $i \in \mathbb{Z}$ so that

$$\begin{aligned} m_i &= f_i + \eta_i \\ &= A \cdot s_i + B + \eta_i. \end{aligned} \tag{1}$$

The pulse shape $s = (s_0, \dots, s_n)$ is approximated by averaging many pulses to obtain the estimate $\hat{s} = (\hat{s}_0, \dots, \hat{s}_n)$, and the noise covariance $r = (r_0, \dots, r_n, \dots)$, given by the expectation

$$r_k = \mathbb{E}[\eta_i \eta_{i+k}] - \mathbb{E}[\eta_i]^2, \tag{2}$$

is approximated by averaging over pulse-free samples of the sensor output to obtain the estimate $\hat{r} = (\hat{r}_0, \dots, \hat{r}_n, \dots)$.

3.2 Algorithm Mean and Variance

A running sum $M_j^L = m_j + \dots + m_{j+L-1}$ beginning with sample j and running for L samples has mean

$$\begin{aligned} \mathbb{E}[M_j^L] &= A \sum_{i=j}^{j+L-1} s_i + L \cdot B + \mathbb{E} \left[\sum_{i=j}^{j+L-1} \eta_i \right] \\ &= A \sum_{i=j}^{j+L-1} s_i + L \cdot B, \end{aligned} \tag{3}$$

and variance

$$\begin{aligned} \text{Var}[M_j^L] &= \mathbb{E}[(M_j^L)^2] - \mathbb{E}[M_j^L]^2 \\ &= \mathbb{E} \left[\left(A \sum_{i=j}^{j+L-1} s_i + L \cdot B + \sum_{i=j}^{j+L-1} \eta_i \right)^2 \right] - \mathbb{E}[M_j^L]^2 \\ &= \sum_{i=j}^{j+L-1} \sum_{k=j}^{j+L-1} \mathbb{E}[\eta_i \eta_k] \\ &= \mathbf{1}^{(L)} \cdot R^{(L)} \cdot \mathbf{1}^{(L)}, \end{aligned} \tag{4}$$

where $R^{(L)}$ is the $L \times L$ covariance matrix with $R_{ij}^{(L)} = r_{|i-j|}$ and $\mathbf{1}^{(L)}$ is the L -vector consisting entirely of ones.

When $j \leq -L$, the pulse contribution $\sum_{i=j}^{j+L-1} s_i$ vanishes and the mean is $L \cdot B$.

With running sum $M_j^{L_{RS}}$ of length L_{RS} within the pulse and running sum M^{L_B} of length L_B for the baseline, the amplitude estimate \hat{A} is defined as

$$\hat{A} = \frac{M_j^{L_{RS}}/L_{RS} - M^{L_B}/L_B}{L_{RS}^{-1} \sum_{i=j}^{j+L_{RS}-1} \hat{s}_i} \tag{5}$$

with approximate mean A and its variance estimate is defined as

$$\hat{\text{Var}}[\hat{A}] = \frac{\mathbf{1}^{(L_{RS})} \cdot \hat{R}^{(L_{RS})} \cdot \mathbf{1}^{(L_{RS})}/L_{RS}^2 + \mathbf{1}^{(L_B)} \cdot \hat{R}^{(L_B)} \cdot \mathbf{1}^{(L_B)}/L_B^2}{(L_{RS}^{-1} \sum_{i=j}^{j+L_{RS}-1} \hat{s}_i)^2}, \tag{6}$$

where $\hat{R}_{ij}^{(L)} = \hat{r}_{|i-j|}$. We have $\mathbb{E}[\hat{A}] = A$ provided $\hat{s} = s$ and $\hat{\text{Var}}[\hat{A}] = \text{Var}[\hat{A}]$ provided in addition $\hat{r} = r$. Under the model, the pulse arrival time is known.

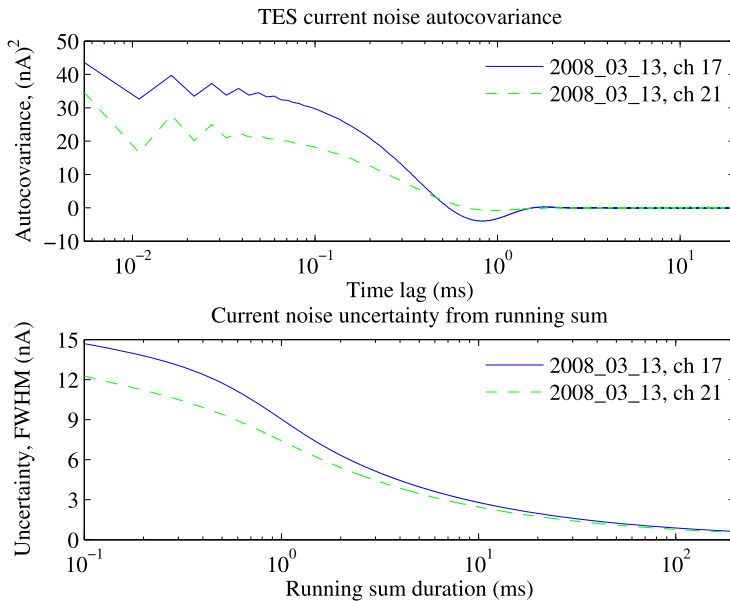


Fig. 1 (Color online) Autocovariance of noise of SQUID-multiplexed TES microcalorimeter detector array, two channels (*top*), is computed here from the power spectral density of source-free data. (For lag 0, the variance is 100.5 (nA)^2 for channel 17 and 100.9 (nA)^2 for channel 21.) Resulting FWHM $\sqrt{8 \log(2) (1^{(L)} C^{(L)} 1^{(L)} / L^2)}$ of the current is obtained from the average of a running sum of length L (*bottom*)

For any choice of L_{RS} , the variance estimate is minimized when the offset j maximizes the denominator and L_B is as large as possible. The optimal choice of L_{RS} depends on the pulse shape and covariance.

4 Experimental Results

To enable quantitative comparison with Hui Tan *et al.* [3], we have used data from the same TES microcalorimeters excited by the same source, although the dates of data collection, 2008/04/11 for the multiplexed 2×4 array, 2008/03/13 for the 2×8 , and 2008/03/26 for the 2×12 , differ somewhat from those presented by Hui Tan *et al.* [3]. Processing of the pulses in 2008 included an optimal-pulse-height-estimation [4] procedure using a typical implementation [5] involving fixed-length digitized records, from which average pulse and noise power spectral density (PSD) for each microcalorimeter were determined.

For the present analysis, the autocovariance was determined from the PSD, according to the Wiener-Khinchin theorem that a function's autocorrelation is the Fourier transform of its PSD. In Fig. 1 the TES current noise autocovariance is shown with the corresponding uncertainty of evaluating an average current by running sum.

The variance (6) in the amplitude estimate depends also on the pulse height captured by the running sum. The average pulse for two of the detectors of the 2×8

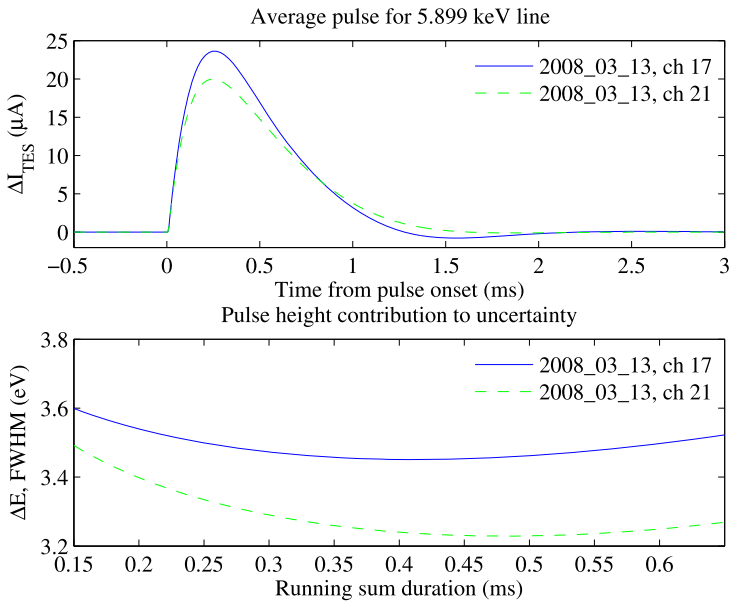


Fig. 2 (Color online) The length L_{RS} of the running sum to determine the pulse height can be chosen to minimize the first of two terms of the variance (6). The average pulse (top) and the noise covariance (Fig. 1) combined lead to minimum variance at running-sum duration 413 μs for channel 17 and 484 μs for channel 21 (bottom). Within this range of durations the sensitivity of the energy resolution to L_{RS} is rather mild

Table 1 Predicted and observed energy resolutions for the running-sum algorithm and optimal filtering are averaged for three microcalorimeter arrays

Avg. res. (eV)	2×4		2×8		2×12	
	RS	Opt	RS	Opt	RS	Opt
Predicted	3.28	2.82	3.28	2.89	3.37	3.02
Observed	3.04	2.71	3.19	2.93	3.35	3.04

array is shown in Fig. 2, together with the dependence of the energy resolution on the length L_{RS} of the running sum.

Comparison of the energy resolution, predicted and observed, for the running sum algorithm (RS) and optimal filtering (Opt) is shown in Fig. 3 and summarized in the Table 1.

5 Discussion

Agreement between predicted and observed energy resolution for the running sum algorithm is generally quite good, despite the analysis ignoring uncertainties of estimating the autocovariance and average pulse, and other issues. The poor agreement for a few detectors, in which predicted resolutions are typically elevated, is likely due in part to undetected stray events in the noise record used for estimating the autocovariance, events that are unimportant in estimation of pulse height.

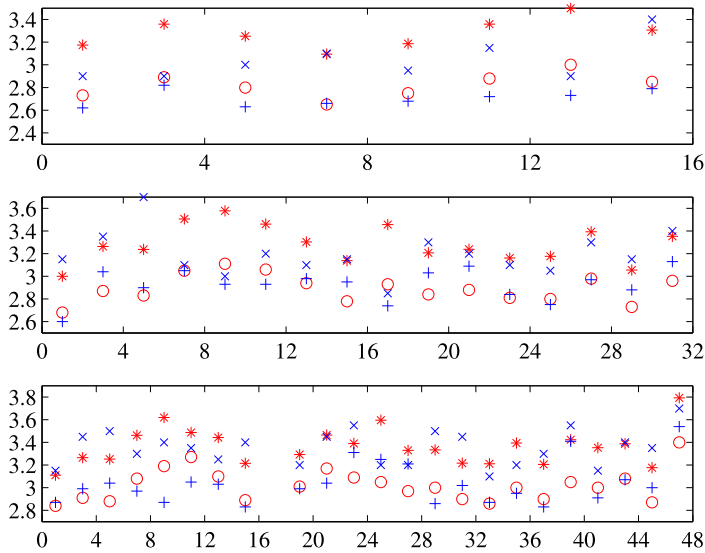


Fig. 3 (Color online) Energy resolution (FWHM, eV) versus detector channel number, for running sum algorithm compared with optimal filtering, predicted and observed, for detectors of 2×4 array (*top*), 2×8 array (*middle*), and 2×12 array (*bottom*). Choice of running sum lengths L_{RS} and L_B for durations of $435.2 \mu\text{s}$ for the pulse and 174.1ms for the baseline, respectively, match those of Hui Tan *et al.* [3]. Legend: running-sum algorithm (*) predicted, (x) observed [3]; optimal filtering (o) predicted, (+) observed

References

1. H. Tan, D. Breus, W. Hennig, K. Sabourov, W.K. Warburton, W.B. Doriese, J.N. Ullom, M.K. Bacrania, A.S. Hoover, M.W. Rabin, in *IEEE Nuclear Science Symp. Conf. Record* (2008), pp. 1130–1133
2. H. Tan, D. Breus, W. Hennig, K. Sabourov, J.W. Collins, W.K. Warburton, W. Bertrand Doriese, J.N. Ullom, M.K. Bacrania, A.S. Hoover, M.W. Rabin, in *AIP Conf. Proc. (American Institute of Physics)*, vol. 1185, ed. by B. Cabrera, A. Miller, B. Young (2009), pp. 294–297
3. H. Tan, W. Hennig, W.K. Warburton, W.B. Doriese, C.A. Kilbourne, *IEEE Trans. Appl. Supercond.* **21**(3), 276–280 (2011)
4. S.H. Moseley, R.L. Kelley, R.J. Schoelkopf, A.E. Szymkowiak, D. McCammon, J. Zhang, *IEEE Trans. Nucl. Sci.* **35**, 59–64 (1988)
5. A.E. Szymkowiak, R.L. Kelley, S.H. Moseley, C.K. Stahle, *J. Low Temp. Phys.* **93**, 281–285 (1993)